

## 20 × 960-Gb/s Space-division-multiplexed 32QAM transmission over 60 km few-mode fiber

**Citation for published version (APA):**

Sleiffer, V. A. J. M., Leoni, P., Jung, Y., Surof, J., Kuschnerov, M., Veljanovski, V., Alam, S. U., Richardson, D. J., Grüner-Nielsen, L., Sun, Y., Corbett, B., Winfield, R., Calabro, S., & Waardt, de, H. (2014). 20 × 960-Gb/s Space-division-multiplexed 32QAM transmission over 60 km few-mode fiber. *Optics Express*, 22(1), 749-755. <https://doi.org/10.1364/OE.22.000749>

**DOI:**

[10.1364/OE.22.000749](https://doi.org/10.1364/OE.22.000749)

**Document status and date:**

Published: 01/01/2014

**Document Version:**

Publisher's PDF, also known as Version of Record (includes final page, issue and volume numbers)

**Please check the document version of this publication:**

- A submitted manuscript is the version of the article upon submission and before peer-review. There can be important differences between the submitted version and the official published version of record. People interested in the research are advised to contact the author for the final version of the publication, or visit the DOI to the publisher's website.
- The final author version and the galley proof are versions of the publication after peer review.
- The final published version features the final layout of the paper including the volume, issue and page numbers.

[Link to publication](#)

**General rights**

Copyright and moral rights for the publications made accessible in the public portal are retained by the authors and/or other copyright owners and it is a condition of accessing publications that users recognise and abide by the legal requirements associated with these rights.

- Users may download and print one copy of any publication from the public portal for the purpose of private study or research.
- You may not further distribute the material or use it for any profit-making activity or commercial gain
- You may freely distribute the URL identifying the publication in the public portal.

If the publication is distributed under the terms of Article 25fa of the Dutch Copyright Act, indicated by the "Taverne" license above, please follow below link for the End User Agreement:

[www.tue.nl/taverne](http://www.tue.nl/taverne)

**Take down policy**

If you believe that this document breaches copyright please contact us at:

[openaccess@tue.nl](mailto:openaccess@tue.nl)

providing details and we will investigate your claim.

# 20 × 960-Gb/s Space-division-multiplexed 32QAM transmission over 60 km few-mode fiber

V. A. J. M. Sleiffer,<sup>1,\*</sup> P. Leoni,<sup>2</sup> Y. Jung,<sup>3</sup> J. Surof,<sup>4</sup> M. Kuschnerov,<sup>5</sup> V. Veljanovski,<sup>5</sup> S. U. Alam,<sup>3</sup> D. J. Richardson,<sup>3</sup> L. Grüner-Nielsen,<sup>6</sup> Y. Sun,<sup>7</sup> B. Corbett,<sup>8</sup> R. Winfield,<sup>8</sup> S. Calabrò,<sup>5</sup> and H. de Waardt<sup>1</sup>

<sup>1</sup>COBRA institute, Eindhoven University of Technology, Netherlands

<sup>2</sup>Universität der Bundeswehr München, 85577 Neubiberg, Germany

<sup>3</sup>Optoelectronics Research Centre, University of Southampton, Southampton, SO17 1 BJ, UK

<sup>4</sup>Technische Universität München, Arcisstr. 21, 80333 München, Germany

<sup>5</sup>Coriant R&D GmbH, St.-Martin-Str. 76, 81541 München, Germany

<sup>6</sup>OFS, Priorparken 680, 2605 Brøndby, Denmark

<sup>7</sup>OFS, 2000 Northeast Expressway, Norcross, Georgia 30071, USA

<sup>8</sup>Tyndall National Institute, Cork, Ireland

[v.a.j.m.sleiffer@tue.nl](mailto:v.a.j.m.sleiffer@tue.nl)

**Abstract:** We show transmission of 20 wavelength-division-multiplexed (WDM) × 960-Gb/s space-division-multiplexed 32QAM modulated channels (spectral efficiency (SE) of 15 bits/s/Hz) over 60 km of few-mode fiber (FMF) with inline few-mode EDFA (FM-EDFA). Soft-decision FEC was implemented and used to achieve error-free transmission.

©2014 Optical Society of America

**OCIS codes:** (060.1660) Coherent communications; (060.2330) Fiber optics communications; (060.4080) Modulation; (060.4230) Multiplexing.

## References and links

1. D. Richardson, J. Fini, and L. Nelson, "Space-division multiplexing in optical fibres," *Nat. Photonics* **7**(5), 354–362 (2013).
2. P. Sillard, M. Astruc, D. Boivin, H. Maerten, and L. Provost, "Few-mode fiber for uncoupled mode-division multiplexing transmissions," in *37th European Conference and Exposition on Optical Communications*, OSA Technical Digest (CD) (Optical Society of America, 2011), paper Tu.5.LeCervin.7.
3. E. Ip, M. Li, Y. Huang, A. Tanaka, E. Mateo, W. Wood, J. Hu, Y. Yano, and K. Koreshkov, "146λ×19-gbaud wavelength- and mode-division multiplexed transmission over 10×50-km spans of few-mode fiber with a gain-equalized few-mode EDFA," in *Optical Fiber Communication Conference/National Fiber Optic Engineers Conference 2013*, OSA Technical Digest (online) (Optical Society of America, 2013), paper PDP5A.2.
4. V. Sleiffer, Y. Jung, B. Inan, H. Chen, R. van Uden, M. Kuschnerov, D. van den Borne, S. Jansen, V. Veljanovski, T. Koonen, D. Richardson, S. Alam, F. Poletti, J. Sahu, A. Dhar, B. Corbett, R. Winfield, A. Ellis, and H. De Waardt, "Mode-division-multiplexed 3×112-Gb/s DP-QPSK transmission over 80 km few-mode fiber with inline MM-EDFA and blind DSP," in *European Conference and Exhibition on Optical Communication*, OSA Technical Digest (online) (Optical Society of America, 2012), paper Tu.1.C.2.
5. S. Randel, R. Ryf, A. Gnauck, M. Mestre, C. Schmidt, R. Essiambre, P. Winzer, R. Delbue, P. Pupaiaikis, A. Sureka, Y. Sun, X. Jiang, and R. Lingle, "Mode-multiplexed 6×20-GBd QPSK transmission over 1200-km DGD-compensated few-mode fiber," in *National Fiber Optic Engineers Conference*, OSA Technical Digest (Optical Society of America, 2012), paper PDP5C.5.
6. R. Ryf, S. Randel, N. Fontaine, M. Montoliu, E. Burrows, S. Chandrasekhar, A. Gnauck, C. Xie, R. Essiambre, P. Winzer, R. Delbue, P. Pupaiaikis, A. Sureka, Y. Sun, L. Gruner-Nielsen, R. Jensen, and R. Lingle, "32-bit/s/Hz spectral efficiency WDM transmission over 177-km few-mode fiber," in *Optical Fiber Communication Conference/National Fiber Optic Engineers Conference 2013*, OSA Technical Digest (online) (Optical Society of America, 2013), paper PDP5A.1.
7. V. A. Sleiffer, Y. Jung, V. Veljanovski, R. G. van Uden, M. Kuschnerov, H. Chen, B. Inan, L. G. Nielsen, Y. Sun, D. J. Richardson, S. U. Alam, F. Poletti, J. K. Sahu, A. Dhar, A. M. Koonen, B. Corbett, R. Winfield, A. D. Ellis, and H. de Waardt, "73.7 Tb/s (96 × 3 × 256-Gb/s) mode-division-multiplexed DP-16QAM transmission with inline MM-EDFA," *Opt. Express* **20**(26), B428–B438 (2012).
8. Y. Jung, V. Sleiffer, N. Baddela, M. Petrovich, J. Hayes, N. Wheeler, D. Gray, E. Numkam Fokoua, J. Wooler, N. Wong, F. Parmigiani, S. Alam, J. Surof, M. Kuschnerov, V. Veljanovski, H. de Waardt, F. Poletti, and D. Richardson, "First demonstration of a broadband 37-cell hollow core photonic bandgap fiber and its application to high capacity mode division multiplexing," in *Optical Fiber Communication Conference/National Fiber Optic Engineers Conference 2013*, OSA Technical Digest (online) (Optical Society of America, 2013), paper PDP5A.3.

9. V. Sleiffer, P. Leoni, Y. Jung, J. Surof, M. Kuschnerov, V. Veljanovski, D. Richardson, S. Alam, L. Grüner-Nielsen, Y. Sun, B. Corbett, R. Winfield, S. Calabrò, B. Sommerkorn-Krombholz, H. von Kirchbauer, and H. de Waardt, "20 × 960-Gb/s MDM-DP-32QAM transmission over 60km of FMF with inline MM-EDFA," in *European Conference and Exhibition on Optical Communication*, OSA Technical Digest (online) (Optical Society of America, 2013), paper We.2.D.2.
10. L. Grüner-Nielsen, Y. Sun, J. Nicholson, D. Jakobsen, K. Jespersen, R. Lingle, Jr., and B. Pálsdóttir, "Few mode transmission fiber with low DGD, low mode coupling, and low loss," *J. Lightwave Technol.* **30**(23), 3693–3698 (2012).
11. Y. Jung, S. Alam, Z. Li, A. Dhar, D. Giles, I. P. Giles, J. K. Sahu, F. Poletti, L. Grüner-Nielsen, and D. J. Richardson, "First demonstration and detailed characterization of a multimode amplifier for space division multiplexed transmission systems," *Opt. Express* **19**(26), B952–B957 (2011).
12. Y. Jung, Q. Kang, V. A. Sleiffer, B. Inan, M. Kuschnerov, V. Veljanovski, B. Corbett, R. Winfield, Z. Li, P. S. Teh, A. Dhar, J. Sahu, F. Poletti, S. U. Alam, and D. J. Richardson, "Three mode Er<sup>3+</sup> ring-doped fiber amplifier for mode-division multiplexed transmission," *Opt. Express* **21**(8), 10383–10392 (2013).
13. V. Sleiffer, Y. Jung, N. Baddela, J. Surof, M. Kuschnerov, V. Veljanovski, J. Hayes, N. Wheeler, E. Numkam Fokoua, J. Wooler, D. Gray, N. Wong, F. Parmigiani, S. Alam, M. Petrovich, F. Poletti, D. Richardson, and H. de Waardt, "High capacity mode-division multiplexed optical transmission in a novel 37-cell hollow-core photonic bandgap fiber," *J. Lightwave Technol.* (to be published).
14. V. Sleiffer, M. Kuschnerov, R. van Uden, and H. de Waardt, "Differential phase frame synchronization for coherent transponders," *IEEE Photonics Lett.* **25**(21), 2137–2140 (2013).
15. R. Pyndiah, "Near-optimum decoding of product codes: block turbo codes," *IEEE Trans. Commun.* **46**(8), 1003–1010 (1998).
16. P. Leoni, V. Sleiffer, S. Calabrò, M. Kuschnerov, S. Jansen, B. Spinnler, and B. Lankl, "On the performance of a soft decision FEC scheme operating in highly non-linear regime," in *Advanced Photonics Congress*, OSA Technical Digest (online) (Optical Society of America, 2012), paper SpTu3A.6.
17. ITU-T Recommendation G.975.1, Appendix I.9 (2004).
18. R. Essiambre, M. Mestre, R. Ryf, A. Gnauck, R. Tkach, A. Chraplyvy, Y. Sun, X. Jiang, and R. Lingle, "Experimental observation of inter-modal cross-phase modulation in few-mode fibers," *IEEE Photonics Lett.* **25**(6), 535–538 (2013).
19. R. Essiambre, M. Mestre, R. Ryf, A. Gnauck, R. Tkach, A. Chraplyvy, Y. Sun, X. Jiang, and R. Lingle, "Experimental investigation of inter-modal four-wave mixing in few-mode fibers," *IEEE Photonics Lett.* **25**(6), 539–542 (2013).

---

## 1. Introduction

Space-division-multiplexing (SDM) has recently received a lot of interest as a potential means to increase the capacity per fiber [1]. One of the flavors of SDM is mode-division-multiplexing (MDM), using multiple modes in few-mode fibers (FMFs) or photonic bandgap fibers (PBGFs) as transmission lanes. FMFs are expected to offer a higher nonlinear tolerance compared to single-mode fibers because the core size typically is larger for these fibers [2]. In PBGFs the light travels mostly in air, therefore achieving ultra-low nonlinear effects. As such, MDM technology ideally opens up the possibility to transmit higher-order modulation formats over longer distances than possible for single-mode fiber, provided few-mode (FM) erbium-doped fiber amplifiers (EDFAs) can provide the same performance as their single-mode (SM) equivalents. Consequently higher spectral efficiencies (SEs) per fiber per mode, giving a direct comparison to single mode fibers, should be permissible.

MDM technology is rapidly evolving showing high transmitted capacities and SE per core, using dual-polarization quadrature phase shift keying (DP-QPSK) [3–5] and DP-16-level quadrature amplitude modulation (DP-16QAM) [6–8] as modulation formats, proving that mode-multiplexing and de-multiplexing is very robust in combination with multiple-input multiple-output (MIMO) digital signal processing (DSP).

In this paper we extend the work presented in [9]. It is shown that the combination of MDM with MIMO-DSP allow for robust transmission of a 32 GBaud SDM-32QAM signal, with an overall bitrate of 960 Gb/s, having high OSNR requirements, over 60km of FMF with inline FM-EDFA. Using FEC, error-free transmission is achieved with an SE of 5 bits/s/Hz per mode, or equivalently a 15 bits/s/Hz SE per fiber. Also the nonlinear penalty for quasi single-wavelength transmission is evaluated by sweeping the combined (over all modes) channel input power.

## 2. Experimental setup

The experimental setup is depicted in Fig. 1. At the transmitter side 48 even, 48 odd channels and a channel under test (CUT) are running at the 50-GHz ITU-grid specified frequencies (191.35 THz to 196.1 THz). From these, 20 channels are selected (Fig. 1(c)) using a wavelength-selective switch (WSS). Because of the high expected error floor for 32 GBaud DP-32QAM, the CUT external cavity laser (ECL) (<100 kHz linewidth) is modulated with pre-generated 32QAM FEC-coded symbols (subsection 2.1) using digital-to-analog converters (DACs) running at 32 GBaud (Fig. 1(a)) driving the in-phase and quadrature port of an IQ-modulator.

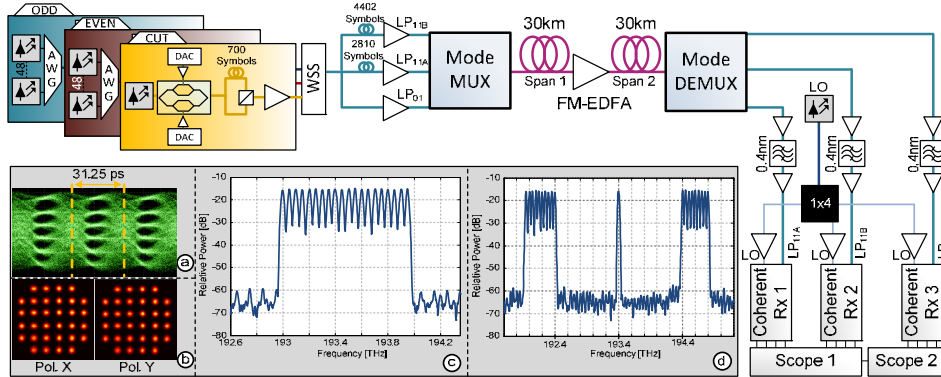


Fig. 1. Experimental setup (a) Electrical driving signal, (b) 320-Gb/s DP-32QAM constellations back to back single mode, (c) Spectrum at transmitter side WDM (20 channels), (d) Spectrum at transmitter side single wavelength.

Subsequently polarization multiplexing was emulated by a polarization multiplexing stage where the incoming signal was split into two equally powered tributaries, after which one of them was delayed by 700 symbols before combining them using a polarization beam combiner (PBC).

The even and odd channels were generated alike except that the electrical signals driving the IQ-modulator were composed of signals created by combining five pseudo random binary sequences (PRBS) of length  $2^{15}$ , for sequence  $n = 2,3,4,5$  shifted by  $4096 \cdot (n-1) - 1$  symbols, and mapped onto 32QAM symbols.

After WDM, the signal is split up into three tributaries, de-correlated with respect to the signal fed to the  $LP_{01}$  port of the mode-multiplexer by 2810 ( $LP_{11a}$ ) and 4402 ( $LP_{11b}$ ) symbols for emulation of separate unique signals, amplified using single-mode EDFAs, and mode-multiplexed (mode MUXed) using a phase-plate based mode MUX [7]. The power was set to + 8.4 dBm per mode (total  $P_{\text{launch}} \sim + 13.1$  dBm).

The transmission link consisted of two 30 km FMF spans supporting the  $LP_{01}$ ,  $LP_{11a}$  and  $LP_{11b}$  modes [10], with fiber details listed in Table 1. The fiber spans are chosen such that the overall differential group delay is averaged out, as observed in Fig. 2(a) by the red and blue lines, trying to minimize the taps needed in the MIMO-DSP. However due to cross-coupling in the FM-EDFA, i.e.  $LP_{01} \rightarrow LP_{11}$  and vice versa, the total spread of the impulse response was around 100 symbols (>201 taps) as explained in Fig. 2(a) by the green and orange line and confirmed by the measured impulse response (corresponding colors) depicted in Fig. 2(b).

Table 1. Fiber Parameters Span 1 and 2

	Length [m]	DGD [ps/m]	MPI [dB]	Disp. $LP_{01}$ [ps/(nm·km)]	Disp. $LP_{11}$ [ps/(nm·km)]	$A_{\text{eff}} LP_{01}$ [ $\mu\text{m}^2$ ]	$A_{\text{eff}} LP_{11}$ [ $\mu\text{m}^2$ ]
Span 1	30000	0.039	-26	19.9	20.1	96	96
Span 2	30000	-0.044	-26	19.8	20.0	95	96

After the first span the signal was amplified using an FM-EDFA [11, 12]. The FM-EDFA pump laser was set to a + 22 dBm pump power to obtain optimal performance [12] at a total input power of  $\sim + 7$  dBm (+ 2.2 dBm per mode). The total output power of the FM-EDFA was  $\sim + 17$  dBm (-4 dB higher than the power launched into span 1).

After mode de-multiplexing (mode DEMUX), described in [7], the signals were amplified using single-mode EDFAs after which the CUT was selected using 50-GHz tunable optical band pass filters. The resulting signals were amplified again before being fed to the coherent receivers employing single-ended photo detectors. An ECL with a linewidth of <100 kHz was divided into three tributaries, amplified with polarization-maintaining single-mode EDFAs yielding +16 dBm signals serving as local oscillators (LOs).

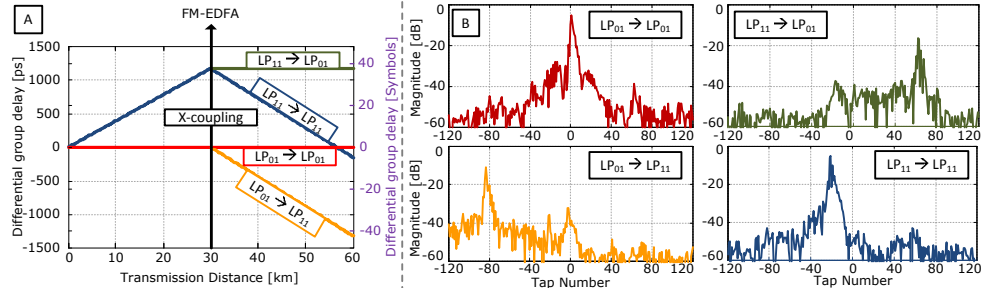


Fig. 2. (a) Differential group delay vs. transmission distance based on Table 1 and cross (X)-coupling in the FM-EDFA. (b) Measured impulse responses after DSP, confirming the prediction from Fig. 2(a).

The coherent receivers 1 and 2, receiving the signals from the LP<sub>11a</sub> and LP<sub>11b</sub> ports respectively, were connected to a 40 GSamples/s digital sampling scope (scope 1) with a 20 GHz electrical bandwidth, whereas the LP<sub>01</sub> port was connected to a 50 GSamples/s digital sampling scope (scope 2) with a 16 GHz electrical bandwidth. Before measuring the scopes were time synchronized by taking into account the delay difference between the ports of the mode DEMUX and the distinct receivers, as well as the delayed trigger signal between the scopes. For the measurements 800,000 samples were collected from scope 1 and 1,000,000 from scope 2. This results in 640,000 symbols available for offline  $6 \times 6$  multiple input multiple output (MIMO) - digital signal processing (DSP).

In the DSP, which is more extensively described in [13], receiver imperfections are removed first. Subsequently the chromatic dispersion is estimated on the LP<sub>01</sub> received signal and compensated for on all signals. After determining the start of the symbols using differential phase correlation technique using BPSK symbols [14], ~100,000 symbols are used for convergence of the data-aided MIMO time-domain equalizer, leaving 500,000 symbols for BER calculation. Three time-different shots are taken per measurement point. The average BER calculated over these measurements is used for displaying the results in the next section.

### 2.1. Hybrid SD/HD FEC scheme

The implemented FEC-scheme consists of a serial concatenation of an inner soft-decision (SD) followed by an outer hard-decision (HD) code [15, 16]. In more detail, the inner code is a turbo product code (TPC) with the extended Hamming (128, 120) code as component code: blocks of  $120 \cdot 120 = 14400$  bits coming from the outer encoder (see below) are placed on a  $120 \times 120$  matrix, and for each row of such matrix 8 bits of redundancy are calculated and appended, thus obtaining a  $120 \times 128$  matrix. Subsequently, the same encoding procedure is applied to the columns (hence, the *product*), including the 8 additional columns previously created, thereby building a  $128 \times 128$  matrix. This process is graphically represented in Fig. 3(a), where the bits to be encoded are indicated with white squares, the redundancy bits resulting from the encoding of rows and columns are reported in grey 25%, and finally those resulting from the encoding of the column of redundancy bits are shown in grey 50%. The encoding along the rows is indicated with orange arrows, while green ones are used to indicate the encoding along the columns. The blocks of  $128 \cdot 128 = 16384$  encoded bits are then taken column wise, divided in groups of 5 bits each and mapped onto 32QAM symbols, as shown in Fig. 3(b).

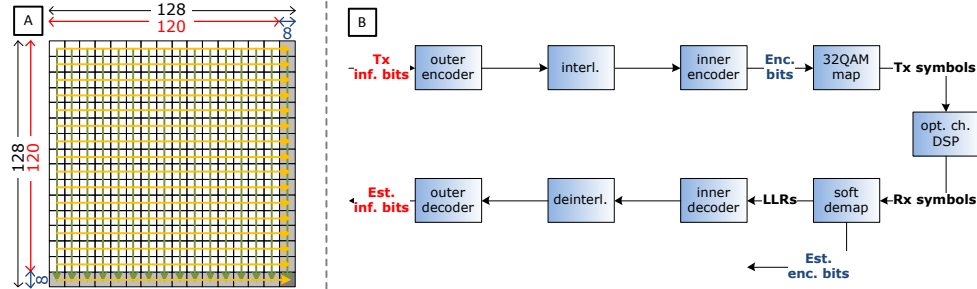


Fig. 3. (a) Graphical representation of the encoding and decoding principle of the inner SD code used in the experiments, and (b) conceptual scheme of the FEC part of the transmitter and receiver (b).

At the receiver, the symbols after DSP are fed to the soft demapper, which calculates the log-likelihood ratios (LLRs) representing the probability of each bit being 1 or 0, given that a certain symbol has been received; clearly, 5 LLRs are calculated for each received symbol. This soft information is then fed to the TPC decoder, where the decoding process introduced in [15] takes place. Similarly to the encoding process at the transmitter, with the help of Fig. 3(a) the decoding process can be explained as follows. The LLRs are placed on a  $128 \times 128$  matrix, and rows are processed first: by exploiting the constraints introduced by the extended Hamming code the LLRs are refined, obtaining a new matrix, of the same size, representing the probability of each bit being 1 or 0, given that a certain symbol has been received and considering the code constraints. Afterwards the same process is applied on the 128 columns of the new matrix (hence, the *turbo*), obtaining a third matrix, again of the same size, containing even more reliable information on the bits. At this point, one decoding iteration has been done. This process can be iterated, resulting in improved performance: we set the number of iterations to 5, a good tradeoff between performance and complexity. After the last iteration the LLRs corresponding to the redundancy bits are discarded, and the sign of the remaining ones is taken as the final binary decision. The TPC has an information word length of  $k = 14400$  and a codeword length of  $n = 16384$ , thus exhibiting a code rate of 0.8789, or equivalently an overhead (OH) of 13.78%. The minimum Hamming distance of the used TPC was  $d = 16$ .

As outer code we considered the one standardized in [17]. Such code has a theoretical threshold of  $3.8 \cdot 10^{-3}$ : if the errors are uniformly distributed, it is able to translate such input bit error rate (BER) to a BER below  $10^{-15}$ , the value typically targeted in optical systems. In practice, the presence of an interleaver of sufficient depth was assumed, and the system was considered error-free when a BER below  $3.8 \cdot 10^{-3}$  was achieved after the inner decoding stage. The inner code was able to achieve such BER when faced with an input BER of  $2 \cdot 10^{-2}$ , which was then assumed as the overall FEC threshold of the system. The outer code has an information word length of 489472 and a codeword length of 522240, thus exhibiting a code rate of 0.9373, or equivalently an OH of 6.69%. Overall, the hybrid SD/HD FEC scheme considered here has a rate of 0.8238, corresponding to an OH of 21.39%.

### 3. Results

Figure 4 depicts all results. Figure 4(a) shows the difference in back-to-back performance between all receivers directly connected (blue) with single-mode fiber to the transmitter, and for the mode MUXed case (red). It can be observed that in the single-mode regime all receivers perform differently, obtaining the worst performance for the receiver connected to the LP<sub>11a</sub> port, with only a very minimal difference at the FEC-limit. This behavior is also observed in the mode MUXed case, however the two receivers receiving the mixed LP<sub>11</sub> modes average out the performance for these modes, obtaining almost the same performance for LP<sub>11a</sub> and LP<sub>11b</sub>, which is observed to be better than the LP<sub>01</sub> performance. The average implementation and mode MUXing penalty are 3.0 dB and 0.7 dB, respectively.



Figure 4(b) shows a comparison between the average back-to-back mode MUXed performance (orange) and the average performance after transmission over 60 km of FMF (blue), as well as the post inner-FEC curve after transmission (purple). The back-to-back curve and the curve after transmission are quasi overlapping, confirming the proper setting of the FM-EDFA. The post inner-FEC curve is showing performance as expected in a single-mode regime, showing proper functioning for MDM transmission. A pre-FEC BER of  $2 \cdot 10^{-2}$  is obtained at an OSNR of 24 dB/0.1 nm. At this point the post inner-FEC BER is already far below the outer-FEC threshold. We verified that each individual tributary achieved an error-free post inner-FEC performance.

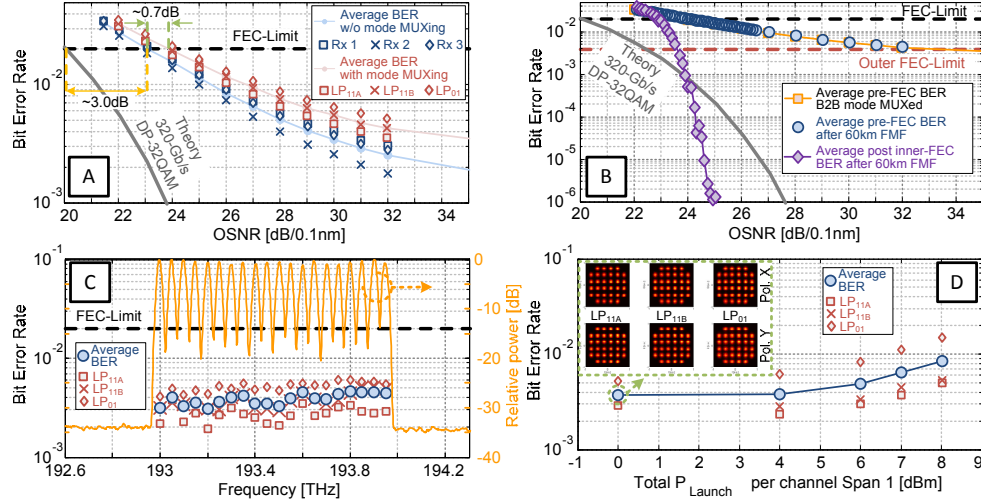


Fig. 4. OSNR vs. BER curves for (a) Single-mode back-to-back (3 receivers) and back-to-back with mode MUXing, (b) back-to-back with mode MUXing and after transmission. (c) Frequency vs. BER for 20 WDM channels after transmission. (d) Nonlinear tolerance measurement for single channel transmission + recovered constellations at a 0 dBm total  $P_{\text{launch}}$ .

The performance after transmission for all the 20 WDM  $\times$  960-Gb/s SDM-32QAM modulated channels and the received spectrum at the LP<sub>01</sub> port are depicted in Fig. 4(c). The received spectrum is flat. To assess the performance of each of the 20 wavelengths, the WSS is used to block one of the odd or even channels and the CUT is tuned and inserted at that wavelength. As can be seen the performance is equal for all channels, showing a maximum average BER around  $5 \cdot 10^{-3}$ , which is well below the FEC-limit, and thus obtaining error-free transmission after FEC-decoding.

Figure 4(d) shows the measurement in which single-wavelength transmission was emulated by selecting neighboring channels on a  $>1$  THz distance from the CUT (Fig. 1(d)). It has been shown that for few-mode fiber transmission inter-modal cross-phase modulation and four-wave mixing can occur between channels separated by several THz [18, 19]. However, the non-linear interactions shown in [18, 19] occur due to the large DGD existing between the LP<sub>01</sub> mode and LP<sub>11</sub> mode, such that the same group velocities are obtained for the signal propagating in the LP<sub>01</sub> mode and the signal propagating in the LP<sub>11</sub> mode when the wavelength difference between the two signals is 16.2 nm ( $\sim 2$  THz). In this paper the DGD between the modes is much smaller, such that the mentioned inter-modal non-linear interactions take place when the wavelengths are separated by  $<5$  nm ( $< \sim 750$  GHz), which depends on the DGD distribution within the FMF [18]. We think however that in this paper the quasi single-wavelength propagation condition should be fulfilled by placing the neighboring channels on a  $> 1$  THz ( $\sim 8$  nm) distance from the CUT. By adding neighboring channels, the launch power of the center channel could be swept, keeping all the overall powers equal such that the FM-EDFA and single-mode EDFAs were performing the same, with the only change in performance arising from nonlinear effects. The figure shows the

total combined power (i.e. all modes) for the CUT as launched into span 1 versus output BER. It should be noted that the power launched into span 2 is  $\sim 4$  dB higher than this power. It is observed that for a total  $P_{\text{launch}}$  of + 6 dBm the performance starts to be affected by nonlinear impairments.

#### **4. Conclusions**

We have shown error-free post-FEC transmission of 20 WDM  $\times$  960-Gb/s SDM-32QAM over 60 km of FMF with inline FM-EDFA. We showed that at a total combined  $P_{\text{launch}}$  of + 6 dBm per channel nonlinear effects start to degrade transmission performance.

#### **Acknowledgment**

This work was supported by the EU FP7-ICT MODE GAP project under grant agreement 258033.